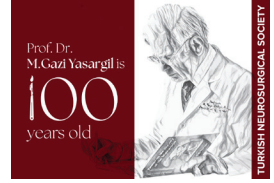




Received: 02.05.2024

Accepted: 20.10.2024

Published Online: 25.06.2025



Original Investigation

General Neurosurgery and
Miscellaneous-Others

Radioanatomical Assessment of the Sphenoid Ridge in Chiari Type I Malformation

Baran Can ALPERGIN¹, Umit EROGLU², Fatih YAKAR³, Umit KARADAGOGLU², Omer Mert OZPISKIN², Elif GOKALP², Muhammet Enes GURSES⁴, Mert CETIN⁵, Orhan BEGER⁶¹Ankara Etlik City Hospital, Department of Neurosurgery, Ankara, Türkiye²Ankara University, Faculty of Medicine, Department of Neurosurgery, Ankara, Türkiye³Pamukkale University, Faculty of Medicine, Department of Neurosurgery, Denizli, Türkiye⁴University of Miami, Miller School of Medicine, Department of Neurological Surgery, Miami, Florida, USA⁵Gaziantep University, Faculty of Medicine, Term V Student, Gaziantep, Türkiye⁶Gaziantep University, Faculty of Medicine, Department of Anatomy, Gaziantep, Türkiye

Corresponding author: Umit EROGLU ✉ umitkovikeroğlu@hotmail.com




ABSTRACT

AIM: To compare the sphenoid ridge (SR) morphology in patients with Chiari type I malformation (CIM) with healthy subjects.**MATERIAL and METHODS:** Three dimensional (3D) computed tomography scans of 49 (25 men / 24 women) CIM patients aged 45.84±18.04 years, and 52 (26 men / 26 women) healthy subjects aged 43.46±11.62 years were included in the investigation. The angulation and dimension of SR were measured for both groups.**RESULTS:** Compared with the controls, CIM patients had greater lesser wing (LW) length ($p<0.001$) and LW width in the midline ($p<0.001$), but shorter LW width in the midpoint ($p=0.001$), LW width in the lateral point ($p<0.001$), and LW angle ($p<0.001$). In CIM, two configurations regarding LW angle types were observed: Type B in 75 LWs (76.5%) and Type C in 23 LWs (23.5%). In controls, two configurations regarding LW angle types were observed: Type A in 35 LWs (33.7%) and Type B in 69 LWs (66.3%). The distribution of the types according to study groups demonstrated that CIM affected significantly LW angle types ($p<0.001$).**CONCLUSION:** LW angle and length may represent middle fossa depth and anterior fossa width, respectively; thus, CIM subjects possess shallow middle fossa and wider anterior fossa.**KEYWORDS:** Chiari type I malformation, Sphenoid bone, Sphenoid ridge, Lesser wing, Computed tomography

INTRODUCTION

The sphenoid ridge (SR), the bony frontier between the anterior fossa and middle fossae, is described as the curved posterior sharp margin of the sphenoid bone's lesser wing (LW) (6,12,14,24). This edge is bounded medially by the anterior clinoid process, and laterally by the pterion, which displays the Sylvian point's approximate position (6,12). Pathologies directly related to SR are rare, but some surgeons report fibrous dysplasia and meningiomas arising from this edge (6). In addition, certain pathologies such as

middle cerebral artery aneurysms may require a surgical procedure, including extensively removal of SR (14). Anatomical information about SR morphology (including its angulation, dimension and shape) may be beneficial for neurosurgeons in avoiding injury to adjacent structures (e.g., orbital branch of the middle meningeal artery, trochlear nerve, superior ophthalmic vein, and oculomotor nerve), when applying surgical procedures such as pterional orbitozygomatic approach or SR keyhole approach (6,8,12,14,24). Moreover, SR may serve as a reference point during these approaches, as this edge forms

Baran Can ALPERGIN  : 0000-0002-3575-0480 Umit KARADAGOGLU  : 0009-0008-6565-102X Muhammet Enes GURSES  : 0000-0001-7141-0654
Umit EROGLU  : 0000-0001-8623-071X Omer Mert OZPISKIN  : 0000-0002-8261-1766 Mert CETIN  : 0000-0002-7165-7646
Fatih YAKAR  : 0000-0001-7414-3766 Elif GOKALP  : 0000-0001-7022-4286 Orhan BEGER  : 0000-0002-4932-8758

This work is licensed by "Creative Commons
Attribution-NonCommercial-4.0 International (CC)".

a border between the frontal and temporal lobes of the brain (14). Therefore, neuroradiologists and neurosurgeons should wise well up to SR morphology to successfully carry out an operation.

Current studies displayed that the whole skull base's osseous components are substantially affected by Chiari type I malformation (CIM), likely resulting from a mesodermal failure (15,22). Nwotchouang et al. observed that such subjects had about 38% bigger sphenoid sinus volume by the side of healthy controls (15). In our opinion, this condition may result major alterations in anatomical properties of structures associated with the sphenoid bone (e.g., LW, sella turcica, and optic canal). For example, CIMs possess smaller sella volume and area, greater angle of the optic canal in axial plane, shorter and wide-angled anterior clinoid process, longer optic strut, longer anterior fossa, and more pneumatized posterior clinoid process by comparison healthy controls (2,4,15-18,22). Differences of skull base morphologies of CIM patients from normal subjects may affect the selection of surgical procedure, intraoperative orientation, and positioning of the patient's head (2,15-18). However, our current knowledge (including morphometric evaluations, precise SR-related anatomical descriptions, and different surgical approach assessments) is mainly obtained from normal subjects (1,8,10,11,14,23,24). Thus, we think that novel studies focused on SR morphology in subjects with different malformations such as CIM are required for determining whether anatomical properties of SR are altered in CIM or not, by comparison healthy individuals. The main goal of our work is to evaluate the angulation and dimension of SR in CIM for improving the present literature data regarding morphometric properties of their cranial base.

MATERIAL and METHODS

Ethics Statement

The Clinical Research Ethics Committee approved ethically our retrospective examination (confirmation no: 2024/97, date: 20.02.2024).

Study Population

Study population was divided into two groups, CIMs and

controls. Patient folders were evaluated to create these groups. Patient files included the following data: complaints, cure methods, radiologic views (CT: computed tomography, and MRI: magnetic resonance imaging), diagnosis procedures, demographic information (gender, age, etc.), and hospital admission/discharge dates.

Inclusion and Exclusion Criteria

Patients were diagnosed as CIM if they had tonsillar herniation over 5 mm downward from the foramen magnum, but no a history of meningocele. In these patients, the circulation of the cerebrospinal fluid was impaired at the level of the foramen magnum. They had balance problems (gait disturbance), and also intense neck pain and vigorous headache, aggravated by Valsalva (sneezing, coughing, straining, etc.). Thus, CIM patients underwent operation, after radiological and clinical diagnosis.

In CIM, inclusion criteria were as follows: a) patients with high-quality preoperative MRI and CT slices, and b) patients diagnosed with CIM after radiological and clinical examinations between 2010-2023. Exclusion criteria were as follows: a) patients with other types of Chiari malformation, b) patients with any disorders regarding the cranial base (e.g., tumor), and c) CIM patients with a history of operation related the anterior and middle fossae.

In controls, inclusion criteria were as follows: a) subjects with high-quality MRI and CT slices, and b) normal subjects. Exclusion criteria were as follows: a) subjects with any malformation or genetic disorder, b) subjects with any disease such as tumors, and c) subjects with a history of medical or surgical treatment related to the skull base.

CT Protocol

The raw data were obtained using a 64-row multidetector scanner (Aquilion 64, Toshiba Medical Systems, Tokyo, Japan). Coronal, sagittal and axial slices were acquired by processing this data. A software (RadiAnt DICOM, Medixant, Poznan, Poland) was used to obtain information about SR.

Measured Parameters

Measurements were performed using 3D CT images (Figure 1).

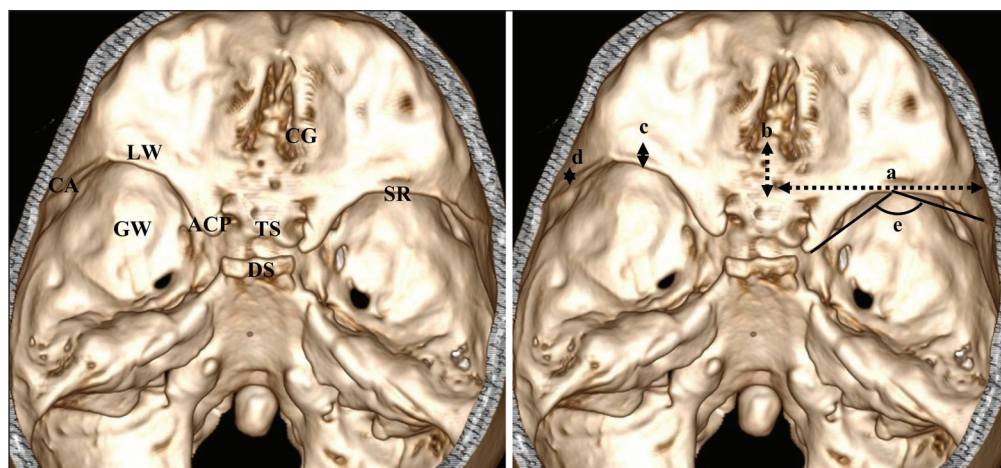


Figure 1: Skull base and measured parameters. **a:** LWL; **b:** LWW-ML; **c:** LWW-MP; **d:** LWW-L; and **e:** LWA; **SR:** sphenoid ridge; **DS:** dorsum sellae; **TS:** tuberculum sellae; **ACP:** anterior clinoid process; **GW:** greater wing; **CA:** crista alaris; **LW:** lesser wing; and **CG:** crista galli.

Considering the previous studies (8, 24), five parameters were measured to obtain data about SR. The explanations of the parameters were as follows: a) LWL: the length of the lesser wing, b) LWW-ML: the width of the lesser wing in the midline, c) LWW-MP: the width of the lesser wing in the midpoint, d) LWW-L: the width of the lesser wing in the lateral tip, and e) LWA: the angle of the lesser wing. Considering the work of Kahilogullari et al. (8), LWA was classified as three types: Type A ($LWA > 130^\circ$), Type B ($130^\circ > LWA > 110^\circ$), and Type C ($LWA < 110^\circ$).

Statistical Analysis

Pearson correlation coefficient test was applied to see correlations between LWL, LWA, LWW-ML, LWW-MP and LWW-L. The student's t-tests were utilized to make gender

(the independent test), group (the independent test), and side (the paired test) comparisons. Chi-square test was utilized to assess relations of LWA types with the study groups. Shapiro-Wilk test was used to assess normality control of the dataset. SPSS (IBM, Armonk, NY) was used to perform statistical evaluations. The " $p < 0.05$ " was considered significant.

RESULTS

CIM group consisted of 49 (25 men / 24 women) patients aged 45.84 ± 18.04 years. Control group consisted of 52 (26 men / 26 women) healthy subjects aged 43.46 ± 11.62 years. Our findings are as follows:

- Compared to the controls, CIM subjects had greater LWL ($p < 0.001$) and LWW-ML ($p < 0.001$), but shorter LWW-MP ($p = 0.001$), LWW-L ($p < 0.001$) and LWA ($p < 0.001$) (Table I).
- In the CIM group, all parameters were similar for sexes and sides ($p > 0.05$). In controls, all parameters except LWA were similar for sexes and sides ($p > 0.05$). Men had greater LWA in comparison with women ($p = 0.008$) (Table II).
- In comparison with control males, CIM males had greater LWL ($p < 0.001$), but shorter LWW-MP ($p = 0.033$), LWW-L ($p < 0.001$) and LWA ($p < 0.001$). By comparison control females, CIM females had greater LWL ($p < 0.001$) and LWW-ML ($p = 0.001$), but shorter LWW-MP ($p = 0.017$), LWW-L ($p < 0.001$) and LWA ($p < 0.001$) (Table III).

Table I: Comparison of CIM and Controls

Parameters	CIM	Controls	p-value
LWL (mm)	52.45 ± 5.25	41.23 ± 8.30	<0.001
LWW-ML (mm)	9.92 ± 1.85	8.75 ± 1.25	<0.001
LWW-MP (mm)	3.08 ± 1.28	3.52 ± 0.45	0.001
LWW-L (mm)	1.88 ± 0.51	2.76 ± 0.69	<0.001
LWA ($^\circ$)	116.42 ± 5.16	126.19 ± 7.73	<0.001

Table II: Sex and Side Comparisons for CIM and Controls

Group	Parameters	Male	Female	p-value	Right	Left	p-value
CIM	LWL (mm)	52.41 ± 5.37	52.50 ± 5.19	0.933	52.03 ± 6.39	52.87 ± 3.83	0.437
	LWW-ML (mm)	9.52 ± 1.53	10.33 ± 2.08	0.124	-	-	-
	LWW-MP (mm)	3.09 ± 1.19	3.07 ± 1.38	0.965	3.12 ± 1.36	3.04 ± 1.20	0.767
	LWW-L (mm)	1.81 ± 0.50	1.96 ± 0.52	0.166	1.86 ± 0.42	1.91 ± 0.59	0.645
	LWA ($^\circ$)	117.32 ± 4.97	115.48 ± 5.24	0.077	116.49 ± 5.63	116.35 ± 4.70	0.892
Controls	LWL (mm)	41.48 ± 8.42	40.98 ± 8.24	0.764	41.49 ± 7.59	40.97 ± 9.01	0.748
	LWW-ML (mm)	8.80 ± 1.31	8.70 ± 1.21	0.773	-	-	-
	LWW-MP (mm)	3.47 ± 0.47	3.56 ± 0.44	0.291	3.62 ± 0.40	3.42 ± 0.48	0.114
	LWW-L (mm)	2.77 ± 0.69	2.76 ± 0.70	0.946	2.46 ± 0.67	3.06 ± 0.58	0.052
	LWA ($^\circ$)	128.17 ± 8.30	124.21 ± 6.61	0.008	126.75 ± 7.95	125.63 ± 7.53	0.464

Table III: Sex Comparison for Both Groups

Parameters	CIM Male	Control Male	p-value	CIM Female	Control Female	p-value
LWL (mm)	52.41 ± 5.37	41.48 ± 8.42	<0.001	52.50 ± 5.19	40.98 ± 8.24	<0.001
LWW-ML (mm)	9.52 ± 1.53	8.80 ± 1.31	0.077	10.33 ± 2.08	8.70 ± 1.21	0.001
LWW-MP (mm)	3.09 ± 1.19	3.47 ± 0.47	0.033	3.07 ± 1.38	3.56 ± 0.44	0.017
LWW-L (mm)	1.81 ± 0.50	2.77 ± 0.69	<0.001	1.96 ± 0.52	2.76 ± 0.70	<0.001
LWA ($^\circ$)	117.32 ± 4.97	128.17 ± 8.30	<0.001	115.48 ± 5.24	124.21 ± 6.61	<0.001

Table IV: Correlations Between the Parameters for CIM and Controls

Group	Parameters	LWW-ML	LWW-MP	LWW-L	LWA
CIM	LWL	-0.038	0.184	0.043	0.056
		0.794	0.070	0.674	0.582
	LWW-ML		-0.165	-0.079	-0.168
			0.258	0.590	0.248
	LWW-MP			0.168	-0.103
				0.098	0.314
	LWW-L				-0.139
Control					0.172
	LWL	0.700**	0.688**	0.588**	0.107
		<0.001	<0.001	<0.001	0.281
	LWW-ML		0.481**	0.159	0.037
			<0.001	0.259	0.794
	LWW-MP			0.217*	0.058
				0.027	0.559
	LWW-L				0.034
					0.733

*: $p < 0.05$, **: $p < 0.01$, Bold values indicate statistically significant correlations.

Table V: Distribution of LWA Types according to Study Groups

Groups	Type A	Type B	Type C	Total	p-value
CIM	0	75 (76.5%)	23 (23.5%)	98	<0.001
Controls	35 (33.7%)	69 (66.3%)	0	104	
Total	35	144	23	202	

- In the CIM group, positive or negative correlations were not found between the parameters. In controls, positive correlations were found between LWL and LWW-ML ($p < 0.001$, $r = 0.700$), between LWL and LWW-MP ($p < 0.001$, $r = 0.688$), between LWL and LWW-L ($p < 0.001$, $r = 0.588$), between LWW-ML and LWW-MP ($p < 0.001$, $r = 0.481$), and between LWW-MP and LWW-L ($p = 0.027$, $r = 0.217$) (Table IV).
- In the CIM group, two configurations regarding LWA types were observed: Type B in 75 LWs (76.5%) and Type C in 23 LWs (23.5%). Type A was not observed in CIM. In controls, two configurations regarding LWA types were observed: Type A in 35 LWs (33.7%) and Type B in 69 LWs (66.3%). Type C was not found in controls. The distribution of LWA types according to study groups was presented in Table V, which displayed that this classification was affected by CIM ($p < 0.001$).

■ DISCUSSION

CIM is described as tonsillar herniation over 5 mm downward from the foramen magnum on MRI (9). It has an incidence of 0.24-3.6% (9). This malformation is considered mainly due to deviations in occipital somite development, arising from the paraxial mesoderm (3). In CIM, osseous components of the posterior fossa are primarily affected and this leads to about 25% reduction in fossa volume (3,21). The most obvious sign of volumetric shrinkage is the overcrowding of the hindbrain, which results in various symptoms (3,9,21). The current investigations show that the whole skull base's osseous components are substantially affected by CIM, likely resulting from a mesodermal failure (15,22). For instance, in comparison with normal subjects, such patients possess longer anterior fossa (22). Similar to CIM, the whole skull base's osseous components are substantially affected by Chiari type II malformation (CIIM) (19). For instance, in comparison with normal subjects, CIIMs had taller pituitary gland with no pathology, longer tuberculum sellae, shorter dorsum sellae, and shallow sella (19). Patel et al. stated that this condition may cause a misinterpretation like the enlargement of the pituitary gland, as the shallow sella may cause the normal gland to appear taller than normal on MRI (19). In these regards, we believe that novel examinations are required for determining whether CIM and CIIM affect morphological properties of anatomical structures like SR present in the anterior fossa and/or middle fossa.

Variations and anomalies of SR and LW have surgical implications (7,8,24). Although rare, the following variations or anomalies have been reported: fusion with the greater wing, absent LW ossification, absent LW, and LW pneumatization (7,24). Lin et al. found that the Sylvian fissure was negatively correlated with SR, and thus a shallow ridge could result in a deep fissure (11). Moreover, abnormalities of the ridge may be related to certain diseases such as Apert syndrome and neurofibromatosis type-1 (7,24). In Apert syndrome, subjects possess perpendicularly angulated SRs (24). When approaching to superior orbital fissure through the pterional technique, LW's removal may require (13). In patients with cerebral aneurysms arising from components of the circle of Willis and especially the middle cerebral artery, neurosurgeons may completely remove SR (i.e., the entire area between the anterior clinoid process and crista alaris) to more easily open the Sylvian fissure and visualize those vessels (14). In addition, LW may be used as a guide to move from lateral to medial when approaching to the cavernous sinus (5). Detailed anatomical definitions, expanded morphometric datasets, novel classifications, and radioanatomic examinations of surgical approaches may be beneficial for neurosurgeons to reduce morbidity - mortality rates (8,10,11,23,24). However, the available literature related to the ridge is primarily based on normal pediatric or adult individuals (1,8,10,24). For this reason, our results may be useful for clinicians to understand anatomical features of the anterior and middle cranial bases in CIM patients.

Substantial differences were found between the measurements of study groups. By comparison controls, CIM patients had greater LWL ($p<0.001$) and LWW-ML ($p<0.001$), but shorter LWW-MP ($p=0.001$) and LWW-L ($p<0.001$). In 180 healthy children aged 1-18 years, Alpergin et al. measured LWW-L, LWW-MP, LWW-ML and LWL as 1.91 ± 0.64 mm, 2.84 ± 0.81 mm, 7.78 ± 1.74 mm, and 28.48 ± 8.15 mm, respectively. They determined that these parameters increased with growth (1). Our measurements in controls were distinctly greater than their pediatric measurements. Tubbs et al. studied on 35 adult dry skulls and 15 adult fixed-cadavers, and measured LWW-L (2 mm), LWW-MP (20 mm), LWW-ML (15 mm) and LWL (right: 40 mm, left: 42 mm) (24). Kizilkanat et al. studied on 42 adult dry skulls, and measured LWW-L (2.6 ± 0.6 mm), LWW-ML (20 ± 2.9 mm) and LWL (left: 44.8 ± 4.2 mm, right: 46.6 ± 4 mm) (10). Our mean values of LWW-L and LWL in controls were compatible with the adult literature data, but our mean values of LWW-ML and LWW-MP in controls were distinctly smaller than the adult literature data (10,24). In both groups, no significant differences were observed between the measurements of the right and left sides, similar to the study of Alpergin et al. (1). In CIM, all parameters were similar for sexes. In controls, LWW-L, LWW-MP, LWW-ML and LWL were similar for sexes, but LWA was greater in men than women. Alpergin et al. observed that LWW-MP were greater in men than women (1). These measurements may aid in estimating the relationship between SR and adjacent structures. For instance, a small ridge can correlate with the proximal Sylvian fissure's lateral deviation (20).

CIM patients ($116.42 \pm 5.16^\circ$) had smaller LWA, compared to controls ($126.19 \pm 7.73^\circ$). Kahilogullari et al. conducted on

40 adult dry skulls, and measured LWA as 118° on the right, and 119° on the left. They also conducted on CT images of 40 patients, and measured LWA as 114.9° on the right, and 116.5° on the left (8). Our mean value of LWA in controls was distinctly greater than their measurements. In CIM, two configurations regarding LWA types were observed: Type B in 75 LWs (76.5%) and Type C in 23 LWs (23.5%). In controls, two configurations regarding LWA types were observed: Type A in 35 LWs (33.7%) and Type B in 69 LWs (66.3%). The distribution of LWA types according to study groups displayed that LWA types was affected by this malformation. CIM patients had distinctly smaller LWA in comparison with controls. Kahilogullari et al. identified three types in dry skulls (Type A: 27%, Type B: 43%, and Type C: 28%) and in CT images (Type A: 26%, Type B: 42%, and Type C: 31%). Interestingly, we did not observe Type C in controls, and Type A in CIM. They determined that SR angle was positively correlated with the middle fossa depth (8). In this regard, we think that CIM patients have shallow middle fossa compared to controls.

CONCLUSION

LWA and LWL may represent middle fossa depth and anterior fossa width, respectively; thus, subjects with CIM possess a shallow middle fossa and a wider anterior fossa.

Declarations

Funding: This research did not receive any specific grant from funding agencies in the public, commercial, or not-for-profit sectors.

Availability of data and materials: Available with the author on request.

Disclosure: The authors declare no competing interests.

AUTHORSHIP CONTRIBUTION

Study conception and design: BCA, UE, FY, MEG

Data collection: UK, OMO, EG

Analysis and interpretation of results: BCA, OB

Draft manuscript preparation: BCA, MC, OB

Critical revision of the article: BCA, UE, FY, MEG

All authors (BCA, UE, FY, UK, OMO, EG, MEG, MC, OB) reviewed the results and approved the final version of the manuscript.

REFERENCES

- Alpergin BC, Eroglu U, Ozpiskin OM, Demiryurek S, Gedikli F, Al Khudari MQMG, Beger O: Anatomical features of the sphenoid ridge in the pediatric population. *Childs Nerv Syst* 40:2287-2294, 2024. <https://doi.org/10.1007/s00381-024-06391-y>
- Alpergin BC, Eroglu U, Zaimoglu M, Kilinc MC, Ozpiskin OM, Erdin E, Beger O: Topographic anatomy and pneumatization of the posterior clinoid process in Chiari type I malformation. *World Neurosurg* 185:e767-e773, 2024. <https://doi.org/10.1016/j.wneu.2024.02.130>
- Aydin S, Hanimoglu H, Tanriverdi T, Yentur E, Kaynar MY: Chiari type I malformations in adults: A morphometric analysis of the posterior cranial fossa. *Surg Neurol* 64:237-241, 2005. <https://doi.org/10.1016/j.surneu.2005.02.021>

4. Bas G, Ozkara E, Ozbek Z, Naderi S, Arslantas A: Sella volume and posterior fossa morphometric measurements in Chiari type 1. *Turk Neurosurg* 33:290-295, 2023. <https://doi.org/10.5137/1019-5149.JTN.40088-22.4>
5. Coscarella E, Baskaya MK, Morcos JJ: An alternative extradural exposure to the anterior clinoid process: The superior orbital fissure as a surgical corridor. *Neurosurgery* 53:162-166, 2003. <https://doi.org/10.1227/01.neu.0000068866.22176.07>
6. Guinto G, Abello J, Félix I, González J, Oviedo A: Lesions confined to the sphenoid ridge: Differential diagnosis and surgical treatment. *Skull Base Surg* 7:115-121, 1997. <https://doi.org/10.1055/s-2008-1058602>
7. Jacquemin C, Mullaney P, Bosley TM: Abnormal development of the lesser wing of the sphenoid with microphthalmos and microcephaly. *Neuroradiology* 43:178-182, 2001. <https://doi.org/10.1007/s002340000455>
8. Kahilogullari G, Uz A, Eroglu U, Apaydin N, Yesilirmak Z, Baskaya MK, Egemen N: Does the sphenoid angle effect the operation strategy? Anatomical and radiological investigation. *Turk Neurosurg* 22:618-623, 2012. <https://doi.org/10.5137/1019-5149.JTN.5790-12.0>
9. Kahn EN, Muraszko KM, Maher CO: Prevalence of Chiari I malformation and syringomyelia. *Neurosurg Clin N Am* 26:501-507, 2015. <https://doi.org/10.1016/j.nec.2015.06.006>
10. Kizilkanat ED, Boyan N, Tekdemir I, Soames R, Oguz O: Surgical importance of the morphometry of the anterior and middle cranial fossae. *Neurosurg Q* 17:60-63, 2007. <https://doi.org/10.1097/WNQ.0b013e318033a5b7>
11. Lin J, Nauta HJ, Olivero W: Anatomical relationships between Sylvian fissure and the sphenoid ridge. *Neurol Res* 23:645-646, 2001. <https://doi.org/10.1179/016164101101198947>
12. MacCarty CS: Meningiomas of the sphenoidal ridge. *J Neurosurg* 36:114-120, 1972. <https://doi.org/10.3171/jns.1972.36.1.0114>
13. Morard M, Tcherekayev V, de Tribolet N: The superior orbital fissure: A microanatomical study. *Neurosurgery* 35:1087-1093, 1994. <https://doi.org/10.1227/00006123-199412000-00011>
14. Nathal E, Gomez-Amador JL: Anatomic and surgical basis of the sphenoid ridge keyhole approach for cerebral aneurysms. *Neurosurgery* 56:178-185, 2005. <https://doi.org/10.1227/01.neu.0000145967.66852.96>
15. Nwotchouang BST, Eppelheimer MS, Bishop P, Biswas D, Andronowski JM, Bapuraj JR, Frim D, Labuda R, Amini R, Loth F: Three-dimensional CT morphometric image analysis of the clivus and sphenoid sinus in Chiari malformation type I. *Ann Biomed Eng* 47:2284-2295, 2019. <https://doi.org/10.1007/s10439-019-02301-5>
16. Ozalp H, Ozgural O, Alpergin BC, Inceoglu A, Ozalp S, Armağan E, Ucar H, Beger O: Analysis of the cranial aperture of the optic canal in Chiari type I malformation. *Turk Neurosurg* 34:1081-1092, 2024. <https://doi.org/10.5137/1019-5149.JTN.45482-23.2>
17. Ozalp H, Ozgural O, Alpergin BC, Inceoglu A, Ozalp S, Armağan E, Ucar H, Beger O: Analysis of the prechiasmatic sulcus in Chiari malformation type I. *World Neurosurg* 175:e1149-e1157, 2023. <https://doi.org/10.1016/j.wneu.2023.04.083>
18. Ozalp H, Ozgural O, Alpergin BC, Inceoglu A, Ozalp S, Armağan E, Ucar H, Beger O: Assessment of the anterior clinoid process and optic strut in Chiari malformation type I: A computed tomography study. *J Neurol Surg B Skull Base* 85:302-312, 2023. <https://doi.org/10.1055/s-0043-57248, 2023>
19. Patel D, Saindane A, Oyesiku N, Hu R: Variant sella morphology and pituitary gland height in adult patients with Chiari II malformation: Potential pitfall in MRI evaluation. *Clin Imaging* 64:24-28, 2020. <https://doi.org/10.1016/j.clinimag.2020.02.014>
20. Sato S, Kashimura H, Akamatsu Y, Fujiwara S, Kubo Y, Ogasawara K: Small sphenoid ridge as a factor associated with laterally deviated proximal Sylvian fissure in patients undergoing pterional craniotomy. *World Neurosurg* 167:e705-e709, 2022. <https://doi.org/10.1016/j.wneu.2022.08.069>
21. Schady W, Metcalfe RA, Butler P: The incidence of craniocervical bony anomalies in the adult Chiari malformation. *J Neurol Sci* 82:193-203, 1987. [https://doi.org/10.1016/0022-510x\(87\)90018-9](https://doi.org/10.1016/0022-510x(87)90018-9)
22. Sgouros S, Kountouri M, Natarajan K: Skull base growth in children with Chiari malformation Type I. *J Neurosurg* 107:188-192, 2007. <https://doi.org/10.3171/PED-07/09/188>
23. Spiriev T, Poulsgaard L, Fugleholm K: One piece orbitozygomatic approach based on the sphenoid ridge keyhole: Anatomical study. *J Neurol Surg B Skull Base* 77:199-206, 2016. <https://doi.org/10.1055/s-0035-1564590>
24. Tubbs RS, Salter EG, Oakes WJ: Quantitation of and measurements utilizing the sphenoid ridge. *Clin Anat* 20:131-134, 2007. <https://doi.org/10.1002/ca.20255>